

# Computationally Efficient Obstacle Avoidance Trajectory Planner for UAVs Based on Heuristic Angular Search Method

Han Chen and Peng Lu\*

**Abstract**—For accomplishing a variety of missions in challenging environments, the capability of navigating with full autonomy while avoiding unexpected obstacles is the most crucial requirement for UAVs in real applications. In this paper, we proposed such a computationally efficient obstacle avoidance trajectory planner that can be used in cluttered unknown environments. Because of the narrow view field of single depth camera on a UAV, the information of obstacles around is quite limited thus the shortest entire path is difficult to achieve. Therefore we focus on the time cost of the trajectory planner and safety rather than other factors. This planner is mainly composed of a point cloud processor, a waypoint publisher with Heuristic Angular Search(HAS) method and a motion planner with minimum acceleration optimization. Furthermore, we propose several techniques to enhance safety by making the possibility of finding a feasible trajectory as big as possible. The proposed approach is implemented to run onboard in real-time and is tested extensively in simulation and the average control output calculating time of iteration steps is less than 18 ms.

## I. INTRODUCTION

Unmanned aerial vehicles(UAVs), especially quadrotors, are increasingly used in field applications due to their flexibility, agility, and flexibility. Autonomous navigation enables the aircraft to be used for missions inaccessible or dangerous to humans or ground vehicles, such as search and rescue, inspection and exploration, monitoring and surveillance. Among these tasks, the trajectory and motion planning module plays a vital role in generating a feasible trajectory for the vehicle online. In an unknown and cluttered environment, drone navigation needs to repeatedly and quickly generate collision-free, dynamically feasible trajectories. Considering that drones often fly faster and the environmental information collected by the sensors on the drones is also changing rapidly, this requires less computational burden but a safe and effective obstacle avoidance algorithm to keep the drones up-to-date in flight. The most important is responding quickly enough to the detected static obstacles, or even moving obstacles. First, the trajectory planner needs to obtain information about obstacles in the environment. In most related studies, obstacles are obtained by using two sensors: lidar or depth binocular camera. Lidars are generally large in size and weight and consume too much energy. Although lidars have higher detection accuracy and more stable obstacle information, they are not suitable for small drones we use. The detection accuracy of the depth camera is sufficient for

The authors are with the Adaptive Robotic Controls Lab (ArcLab), Hong Kong Polytechnic University, Hung Hom, Kowloon, Hong Kong, China. [stark.chen@connect.polyu.hk](mailto:stark.chen@connect.polyu.hk); [peng.lu@polyu.edu.hk](mailto:peng.lu@polyu.edu.hk)

\*corresponding author

UAV obstacle avoidance within a certain distance (0.5-8m), but the field of view is narrow, and it is impossible to obtain 360° environmental information like lidar. So we need to use the information obtained by the depth camera to build a global map, which can prevent the drone from hitting obstacles outside the field of view. The accuracy and stability of maps built online is key to avoiding obstacles.

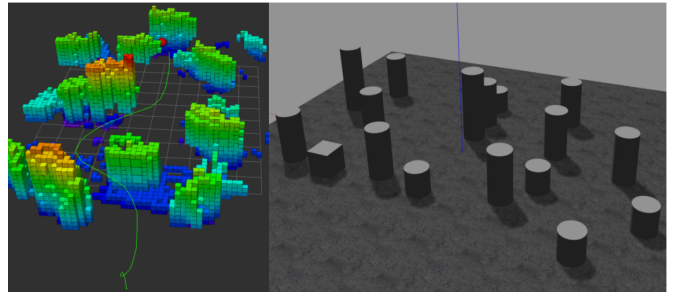


Fig. 1. Our simulation environment and visualized data of results

In this paper, we propose a method to directly find the target point of the drone in the next step on a sparse point cloud, and then solve the optimization problem to obtain the motion primitives that the drone needs to perform at the next moment. In order to reduce the amount of calculation for collision detection when searching for a waypoint, we further streamline the point cloud of obstacles in the global map maintained by Octomap. The degree of simplification is related to the drone safety radius  $rsafe$  we set. Then the discrete angular search is used to simplify the collision detection to calculate the distance from the point to the straight line.

In summary, the main contributions of the paper are as follows:

- A framework that ensures the feasibility of the entire collision avoidance algorithm and guarantees safety, which can work out the motion primitives (acceleration for this paper) as flight control output in a much shorter time than most of the other former similar work.
- The combination of a streamlined point cloud of global Octomap and the heuristic discrete angular search make the computation load of finding a collision-free path become much lighter. It improves the efficiency by generating waypoints directly on the point cloud rather than building a grid map and running a static path planning algorithm (such as A\* or JPS) on the grid map afterward.
- The collision check can be removed from the motion

planning part due to the introduction of *rsafe* and the constraint of maximum speed and acceleration of drone, the drones position can be well constrained in the free space between the execution time of two contiguous steps of the trajectory planner.

- We propose three techniques to guarantee safety in the autonomous flight based on the mentioned method. Simulation experiments in ROS/Gazebo showing agile flights in completely unknown cluttered environments, with maximal average control output calculating time of iteration steps less than 18 ms.

## II. RELATED WORK

At present, algorithms used in UAV route planning can be classified into two categories by whether or not it can be used in real time calculating in an unknown environment. As for static route planning algorithms based on known threats, there are the Voronoi diagram, Dijkstra, A\*, RRT and evolutionary algorithm(EA)[1]. As for dynamic route search algorithms based on unknown threats, there are D\*, VFH, DWA and APF[1].These are all classical methods in path planning and obstacle avoidance but their original version can not be applied in real UAV hardware experiments directly. Though they can work well in a simple 2D map, it is a more complex problem for a UAV with single depth camera flying in the unknown environment. For hardware experiments, it is necessary to encode and use the information of detected obstacles in an efficient way. And for UAVs experiment, especially the quadrotors, the fast reaction, the high security, and the appropriate motion planning method are highly needed and considerable, because the flying speed and dangers are relatively higher and the attitude stability is lower than ground vehicles.

In most of the related research, point cloud is the most widely used format to express obstacle information. For the use of point clouds, the most common practice is to use a filtered point cloud to create a three-dimensional grid map and then perform trajectory planning on the basis of the grid map. Considering the estimation of the vehicle state, many methods have been proposed to convert the depth measurements generated by the on-board sensors into a global map.Representative methods include voxel grids [2], Octomap [3], and elevation maps[4]. Each method has advantages and disadvantages in a particular environment. The voxel grid is suitable for fine-grained representation of small volumes, but the storage complexity is poor. Elevations are suitable for representing artificial structures composed of vertical walls but are less efficient in describing natural and unstructured scenes. Octomap is memory-efficient when indicating an environment with a large open space. This storage structure is very useful for further utilizing maps for trajectory planning and has the function of automatic map maintenance, which is convenient to use and has satisfactory results in both simulation and hardware flight tests.

In the previous work [5] , they use Octomap build on point cloud raw data to develop their own method and gained good experimental results. In another way, in order

to reduce the time consumed by this step of building the map, some researchers have directly planned the trajectory on the original point cloud. Lopez used the transformed point cloud for the collision check with trajectories corresponding to the randomly generated motion primitives[6]. However, planning on the point cloud directly requires high-quality point cloud information, and this method is not suitable for drones carrying a single depth camera if a global map is not established.

After getting the environmental information, the most important thing is to calculate motion primitives. The related methods can also be divided into two categories. One is to first convert the obstacle information and the position of the UAV in three-dimensional space into a local map. This map contains only the obstacle information near the UAV, the global goal and the points of obstacles are converted in this local map in some way, then a static path planning algorithm is run on the local map, and finally the motion primitives are obtained by solving the motion planning equations. For instance, [7]-[8] built a local occupancy grid map with the most recent perception data and generated a minimum-jerk trajectory through waypoints from an A\* search. As for waypoint time allocation, an approximate method was used in [9] and a bi-level optimization was used in [10]-[11] to find the times. Another method is to skip searching paths on the map first and directly generate motion primitives by sampling. Then the evaluation function can be designed to select the most suitable group of motion primitives as the output, which is very similar to DWA. A representative work is presented by Mueller et al, making the quadrotor can even catch a falling ball[12].

In addition, you can also directly obtain motion primitives by solving an optimization problem. This requires appropriate expressions of the trajectory of the aircraft, such as Bezier curves, and to ensure that the final trajectory is collision-free by setting constraints. [13]-[15] achieved satisfactory results by utilizing this method. For these two methods, the collision check is the most time-consuming, and it is difficult to significantly increase the calculation speed within its own framework, so we propose another idea to improve the calculation speed.

## III. QUICK RESPONDING AND SAFE PLANNER

As mentioned above, the collision check is the most time-consuming part of the trajectory generation. To cope with this challenge, we introduce a Heuristic Angular Search(HAS) method with a backup safety plan. The whole algorithm is given as **Algorithm 1**. We describe Line 2-4 in section A and describe Line 5 in Section B. Line 6-7 is described in Section C and Line 9 is described in Section D. Overall, the outer loop can be executed at 55-100 Hz, considering the different source code type and hardware platform performance.

### A. Processing the point cloud

The point cloud data obtained by a real depth camera is often noisy and too dense, and the noise is greater on objects farther from the camera, as shown in Fig. 2(b). This

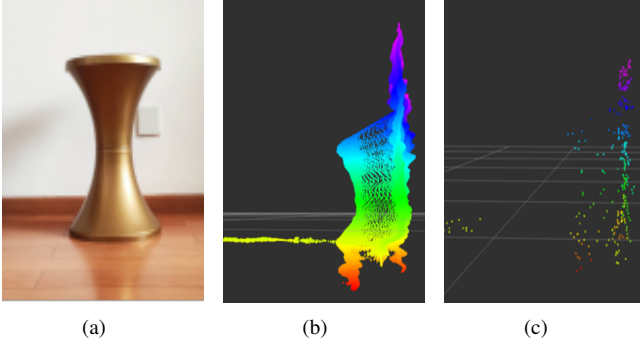


Fig. 2. (a): depth cameras RGB output, (b): raw point cloud, (c): filtered point cloud(Pcl2)

is inconvenient for converting the coordinate system of each point in the point cloud and establishing a global map. First, we filter the original point cloud data  $Pcl1$  through three filters in order to obtain the point cloud data  $Pcl2$  which is convenient to store and recall. The algorithm of the filter and the point cloud after filtering are shown in **Algorithm 2** and Fig. 2(c).  $n_{in}$  is the number of points in  $Pcl1$  whose distance to  $pointk$  is smaller than  $d_v$ ,  $S_d$  is the detected space by a depth camera,  $d_v$ ,  $d_{f1}$ ,  $d_{f2}$ ,  $n_v$ ,  $d_{use}$  are parameters. It can be seen that the filtered point cloud data are more concise and tidy, retaining the basic shape of the obstacle. Then we convert the point cloud into the earth coordinate system and use Octomap to build and maintain a global map. In fact, it is tolerable as long as the gap between the midpoints of the point cloud corresponding to an obstacle is not greater than the safe radius  $r_{safe}$  of the drone, but if you do this for the first time, the global map after fusion will be unavailable for visualizing. So we filter again after we get the point cloud of the global map, the algorithm is also shown in Algorithm 2.  $q$  is one of the three axes value of a point in  $Pcl4$ ,  $L_q$  is the list of distinct  $q$  values of points in  $Pcl4$ ,  $B_E$  is the transformation matrix from body coordinate to earth coordinate,  $c()$  is short for  $\cos()$  and  $s()$  is short for  $\sin()$ , are Eular angles corresponding to  $x, y, z$  axis respectively.

At last, we only use the point in  $Pcl5$  for collision detection.

$$B_E = \begin{bmatrix} c\theta c\psi & s\phi s\theta c\psi - c\phi s\psi & c\phi s\theta c\psi + s\phi s\psi \\ c\theta s\psi & s\phi s\theta s\psi + c\phi c\psi & c\phi s\theta s\psi - s\phi c\psi \\ c\theta s\psi & s\phi c\theta & c\phi c\theta \end{bmatrix}^{-1} \quad (1)$$

$$\begin{aligned} P_{d1} &= l_d (c(\alpha_{g0} + \alpha_d), s(\alpha_{g0} + \alpha_d), s(\beta_{g0})) \\ P_{d2} &= l_d (c(\alpha_{g0} - \alpha_d), s(\alpha_{g0} - \alpha_d), s(\beta_{g0})) \\ P_{d3} &= l_d (c(\alpha_{g0}), s(\alpha_{g0}), s(\beta_{g0} + \alpha_d)) \\ P_{d4} &= l_d (c(\alpha_{g0}), s(\alpha_{g0}), s(\beta_{g0} - \alpha_d)) \end{aligned} \quad (2)$$

$$A_{g0} = \begin{cases} A_g \text{ (others)} \\ A_{last} (\lambda n_{obs} > n_{average}) \end{cases} \quad (3)$$

$$\lambda = \frac{\text{count ( if } A_g = A_{last} \text{ in last 3 steps )}}{3} \quad (4)$$

### Algorithm 1 our proposed planner

---

```

1: while true : do
2:   Filter the raw point cloud data, output Pcl1
3:   Transform Pcl1 in body coordinate (B) to Pcl2 in
   earth coordinate(E)
4:   Build a global map represented by point cloud Pcl3,
   filter again
5:   Find the next waypoint  $N_k$  by heuristic angular search

6:   if found a feasible waypoint: then
7:     Run the minimum acceleration motion planner to
     get motion primitives
8:   else
9:     Run the backup plan for safety, then go to 5
10:  end if
11:  Send the motion primitives to the UAV flight controller
12:  Record the current position  $p_n$  in list  $P_{rec}$ 
13: end while

```

---

### B. Heuristic angular search method

Different from the previous work in which a complete path needs to be planned on the local map, we only find a target point close to the drone in the path planning part as a guide for motion planning. Nonetheless, because the overall planner's calculation speed is quite fast, such a short predicted trajectory is sufficient to refresh before the drone flight reaches its endpoint. As shown in Fig. 3, we use the vector  $A_g = (\alpha_g, \beta_g)$  to represent the angle of the navigation target  $G = (x_g, y_g, z_g)$  relative to the current position of the drone  $p_n(x, y, z)$  in  $E$ . Based on this, we define a series of line segments with different endpoints  $P_{d1}-P_{d4}$ , and these line segments have a common endpoint  $p_n$ .

Algorithm 3 reveals the process of searching for waypoints. We simplified the calculation of collision detection by calculating the vertical distance from a point to a line segment, rather than the distance from the obstacle to the sampled curvy path[16]. The specific process of collision checking is shown in Algorithm 4. In most cases in simulation tests, collision detection can be done within 16ms. The meaning of heuristic search is that the starting point of the search is calculated according to the historical record of the results obtained by this method and the current point cloud information, so as to obtain an initial value  $A_{g0}$  which is the closest to the final search result, minimize the search time cost. The initial value of  $A_{g0}$  is calculated in (3), where  $l_d$  is the detection radius of UAV for obstacle avoidance check,  $\mu$  is a relatively small coefficient with a value between 0.1-0.2.  $A_{last}$  is the angle corresponding to the waypoint in the last step,  $n_{obs}$  is the size of  $Pcl5$  in the current step and  $n_{average}$  is the average of the size of  $Pcl5$  over all past steps.

### C. Motion planning

After getting the path point, the next step is to calculate the control command, such as position  $p = (p_x, p_y, p_z)$ , speed  $v = (v_x, v_y, v_z)$ , acceleration  $a = (a_x, a_y, a_z)$ , and

---

**Algorithm 2** point cloud filter

---

```

1:  $Pcl1 \leftarrow$  point cloud raw data
2: for  $point_i$  in  $Pcl1$  do
3:   if  $\|point_i\|_2 < d_{f1}$  or  $\|point_i\|_2 > d_{f2}$  then
4:     Delete  $point_i$  from  $Pcl1$ 
5:   end if
6: end for
7: for  $voxel_j \in S_d$  do
8:   if any points of  $Pcl1$  is in  $voxel_j$  then
9:     Replace these points with the center of  $voxel_j$ 
10:   end if
11: end for
12: for  $point_k$  in  $Pcl1$  do
13:   if  $n_{in} < n_v$  then
14:     Delete  $point_k$  from  $Pcl1$ 
15:   end if
16: end for
17:  $Pcl2 \leftarrow Pcl1$ 
18: for  $point_m$  in  $Pcl2$  do
19:    $point_m = point_m + p_n$ 
20: end for
21:  $Pcl3 \leftarrow$  center points of Octomap, with  $Pcl2$  input
22:  $Pcl4 \leftarrow Pcl3$ 
23: for  $q_{in}x, y, z$  do
24:   for  $q_w$  of  $point_w$  in  $L_q$  do
25:     if  $not((q_w - L_q(0, q)) \% r_{safe} \approx 0$  or  $[q_w, q_w + r_{safe}]$  not in  $L_q$ ) then
26:       Delete  $point_w$  from  $Pcl4$ 
27:     end if
28:   end for
29: end for
30:  $Pcl5 \leftarrow Pcl4$ 
31: for  $point_t \in Pcl5$  do
32:   if  $\|p_u point_t\|_2 > d_{use}$  then
33:     Delete  $point_t$  from  $Pcl5$ 
34:   end if
35:    $d_{min} = \min(\|p_u point_t\|_2)$ 
36: end for

```

---

send the command to the flight controller, so as to ensure that the aircraft can fly within its own kinematic limit and reach the next waypoint. Generally, the motion primitives are obtained by solving an optimization problem. In this way, the kinematic constraints of the drone can be addressed by setting constraints[17]. We take the acceleration of the drone as the variable to be solved, because compared with the use of jerk or snap, acceleration can be directly sent to the flight control as a control command, and the calculation load is less while meeting the kinematic constraints and ensuring the smooth trajectory.

The optimization problem is defined in (5), where the subscript  $n$  presents the current step in a rolling process of the whole planner,  $p_{start}$  is the position of the drone when the planner starts to work[18].  $v_{max}$  and  $a_{max}$  are the kinematic constraints for speed and acceleration respectively,  $t_{max}$  is the upper bound for the time which can be used to

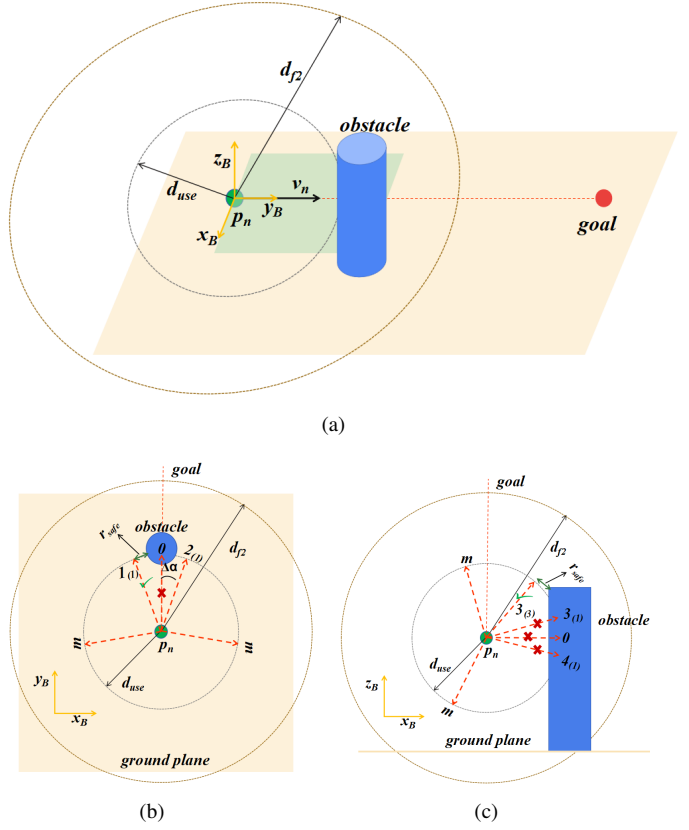


Fig. 3. Illustration about angular search,(a) is a stereogram,(b) and (c) are the projection of (a) to different plane.  $\mathbf{B-xyz}$  presents the body coordinate. The number in the blanket is the ordinal number of iteration, for example,  $2_{(1)}$  presents  $P_{d2}$  with  $\alpha_d = \Delta\alpha$ .

finish the predicted piece of trajectory.  $tol$  is the tolerance for the difference between the end of the predicted trajectory and the  $w_p$ ,  $v_{n+1}$  and  $p_{n+1}$  are calculated by the kinematic formula.

$$\begin{aligned}
 & \min_{a_n, t_n} \|a_n\|_2^2 + \eta t_n \\
 & \text{s.t. } p_0 = p_{start} \\
 & 0 < t_n \leq t_{max} \\
 & v_n = \dot{p}_n \\
 & a_n = \dot{v}_n \\
 & \|v_{n+1}\|_\infty \leq v_{max} \\
 & \|a_n\|_\infty \leq a_{max} \\
 & \|p_{n+1} - \text{waypoint}\|_2 \leq tol \\
 & v_{n+1} = v_n + a_n t_n \\
 & p_{n+1} = p_n + v_n t_n + \frac{1}{2} a_n t_n^2
 \end{aligned} \tag{5}$$

#### D. Safety guarantee

Next, we demonstrate the safety of the trajectory and add additional measures to improve safety based on the above method. As shown in the Fig. 4, if the trajectory of the aircraft is a straight line that coincides with the  $p_n w_p$  in each step, then this line must be safe because it has undergone collision detection. However, considering

---

**Algorithm 3** HAS method

```

1: for  $i$  in 1,2,3,4 do
2:   for  $d$  in  $0, \Delta\alpha, 2\Delta\alpha \dots m\Delta\alpha$  do
3:     if  $d_{Pdi} > r_{safe}$  then
4:        $w_p = \mu P_{d1}$ 
5:       Break all circle
6:     end if
7:   end for
8: end for

```

---

**Algorithm 4** collision check

```

1: for  $point_t$  in  $Pcl5$  do
2:   if  $\|p_{upoint_t}\|_2^2 \leq \|p_{dipoint_t}\|_2^2 + \|p_{dipu}\|_2^2$ 
   or  $\|p_{dipoint_t}\|_2^2 \leq \|p_{upoint_t}\|_2^2 + \|p_{dipu}\|_2^2$  then
3:      $d_{Pdi} = \infty$  (Foot drop of  $point_t$  is not on  $p_{updi}$ )
4:   else
5:      $d_{Pdi} = \frac{\|p_{upoint_t} \times p_{updi}\|_2}{\|p_{updi}\|_2}$ 
6:   end if
7: end for

```

---

the kinematic constraints of the aircraft, the trajectory of the aircraft in each step is a curve. Assuming that the acceleration  $a_n$  solved by the optimizer is in the same plane as the speed  $v_n$  and the waypoint of the drone at the current moment (so that it meets the optimization objective function), then this curve is a parabola in this plane. When  $a_n$  is the opposite of  $v_n$ , the deviation  $d_{max}$  between the drone trajectory and line segment  $p_n w_p$  is the largest. And it can be easily proven since  $\|v_n\|_2$  and  $\|a_n\|_2$  is constant.

$$d_{max} = \max \left( \frac{2 \|v_n\|_2^2}{\|a_n\|_2} \right) \quad (6)$$

$$s.t. \sqrt{\frac{2 \|w_p - p_n\|_2}{\|a_n\|_2}} + \frac{\|v_n\|_2}{\|a_n\|_2} \leq t_{max}$$

We can get  $d_{max}$  by solving this optimization problem:

$$d_{max} = 2 \|v_n\|_2 \left( t_{max} - \sqrt{\frac{2 \|w_p - p_n\|_2}{a_{max}}} \right) \quad (7)$$

The trajectory is safe when we choose parameters to make  $d_{max} < r_{safe}$ . Besides, we have another three techniques to achieve further security (they are further described in Algorithm 5):

- 1) Change  $l_d$  to a smaller one when no feasible  $w_p$  is found at the first circle and run another circle.
- 2) Change  $v_{max}$  to a smaller one when  $d_{min}$  is smaller than  $1.5r_{safe}$  [19].
- 3) If no feasible  $w_p$  is found, return to the last path point and use the next feasible solution in the angular search.

#### IV. EXPERIMENTAL RESULTS

##### A. Experimental Configuration

Our proposed HAS-based trajectory planner was tested and verified in the Robot Operation System (ROS)/Gazebo

---

**Algorithm 5** collision check

```

1:  $i = 1$ 
2: for  $point_t$  in  $Pcl5$  do
3:    $l_d = \varepsilon l_d$ 
4:   if angular search method (use the  $i$ th  $w_p$  found) return  $w_{p(n)}$  then
5:     Break current circle
6:   end if
7: end for
8: if no  $w_{p(n)}$  is found then
9:   Fly to  $p_{n-1}$ 
10:  if  $i < 5$  then
11:     $i = i + 1$ 
12:    Return to line 2
13:  else
14:    Land on ground
15:  end if
16: end if
17: if  $d_{min} < 1.5r_{safe}$  then
18:    $V_{max} = V_{max}d_{min}/1.5r_{safe}$ 
19: end if
20: Run the motion planner

```

---

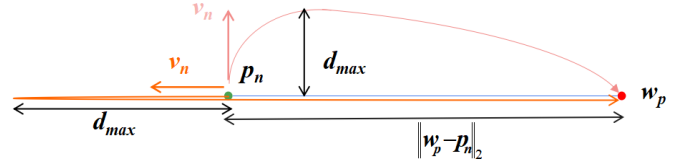


Fig. 4. When  $\|v_n\|_2$  and  $\|a_n\|_2$  is fixed, the predicted trajectory is related to the direction of  $v_n$ .

simulation environment. Gazebo is a simulation software which can provide a physical simulation environment close to the real world, and by modifying the model in the PX4 package in ROS, you can load drone configurations in Gazebo that are almost the same as the equipment used in the hardware experiment: including the rack model, depth camera model, flight control firmware version. The model of the drone we use in the simulation is IRIS, the depth camera model is Kinect V2, and the PX4 1.7.4 firmware version is used as the underlying flight controller. Mavros package is deployed for establishing the communication between our planner node and the PX4 control module. The speed controller for tracking is provided by the PX4 module by default. The point cloud processor is executed by C++ code. In order to show the calculation speed advantage of the planner's HAS method, the other parts are executed by Python scripts. All these timing breakdowns were measured using an IntelCore i7-8200U 1.8GHz Processor. Table I describes the parameter settings of the planner in the simulation test. To make the depth camera observe the environment more efficiently, we control the yaw angle of the drone to keep the camera always heading toward the goal during the flight.

Two flight tests of increasing difficulty are presented in

TABLE I  
PARAMETERS FOR SIMULATION

Parameter	Value	Parameter	Value
$\Delta\alpha$	$10^\circ$	$d_v$	0.5m
$d_{f1}$	0.5m	$n_v$	12
$d_{f2}$	8m	$d_{use}$	3m
$a_{max}$	$4m/s^2$	$r_{safe}$	0.8m
voxel size	0.2m	$v_{max}$	3m/s
$tol$	0.01m	$\mu$	0.1
$l_d$	3m	$d_{max}$	$0.68m < r_{safe}$
$t_{max}$	0.5s	$\eta$	1.2

section B and section C to show the planning trajectory in 3D space and the time cost of each planning step. The obstacles are not known a priori and are unobservable at takeoff.

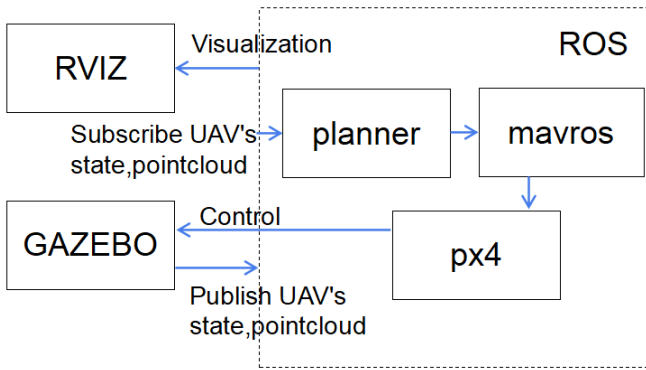


Fig. 5. The relationship among the software for simulation.

### B. Simulation flight test in a simple environment

The tests are shown in the Fig. 6. In the first flight, the starting point of the drone is (0,0,0), and the red point indicates the navigation target point (12,0,1). After reaching the target point, set the starting point change to (12,0,0) and the endpoint is set to (0,0,1), then another test is performed. This is to test the drone's ability to avoid obstacles in the horizontal and vertical directions. According to the design of the algorithm, the drone will choose the path with the smallest amount of angle change of the flight direction when the obstacle can be avoided both horizontally and vertically. Because turning the drone too fast will increase the noise of the point cloud data obtained by the depth camera and destroy the established map, the attitude angle of the drone should be kept as stable as possible.

The global map established by the depth camera on the drone and the flight trajectory of the drone during the flight are displayed in RVIZ, as shown in Fig. 6(c)-(d). In the first flight, the drone first raised its height to avoid the obstacles in the face of short obstacles and then chose to fly to the left to avoid the higher obstacles. In the second test, the drone first chose to fly to the left and then chose to continue to the left, because this minimizes the amount of angle change in the flight direction.

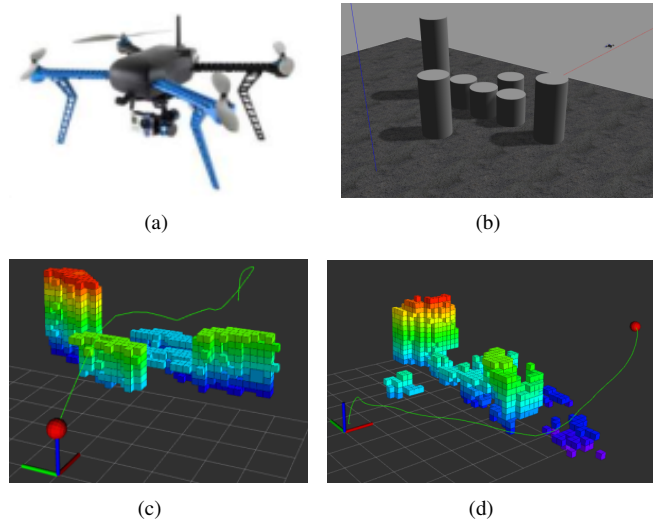


Fig. 6. (a) is an IRIS drone, (b) is a simple simulation environment, (c) and (d) show the results of the first and second flight test. The trajectory is shown in the green line.

### C. Simulation flight test in a complex environment

In this test, we built a relatively complex map. Due to the limited space in the paper, we show only one flights results. The start point is set at (12,0,0), the endpoint is set at (-12,0,1). The flight trajectory of the drone and the established global map are shown in Fig. 7. After repeating the flight experiments 10 times, the detailed data of the trajectory and the average running time of each part of the planner are shown in Fig. 8. TABLE II compares the calculation time of our proposed planner to the state-of-the-art, we can see that our proposed planner has obvious advantages in calculation time.

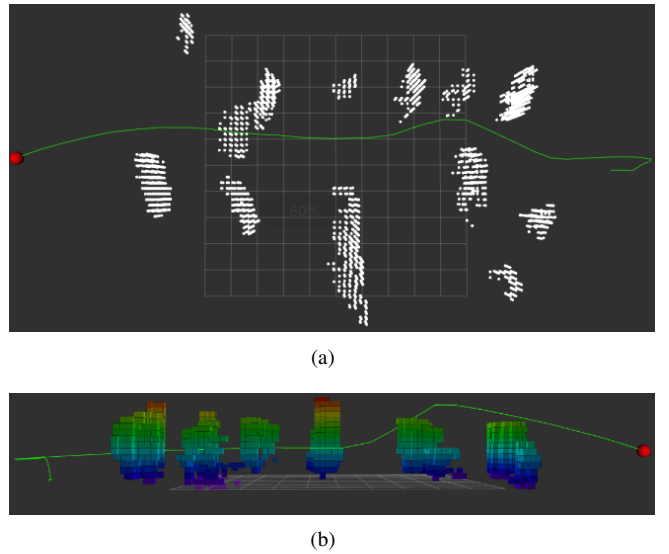


Fig. 7. Results of the test in a complex environment. (a) shows the point cloud of the global map from a high angle and (b) shows the Octomap from a side view.

In Fig. 8(b)-(c), the curve changes intensely near the end

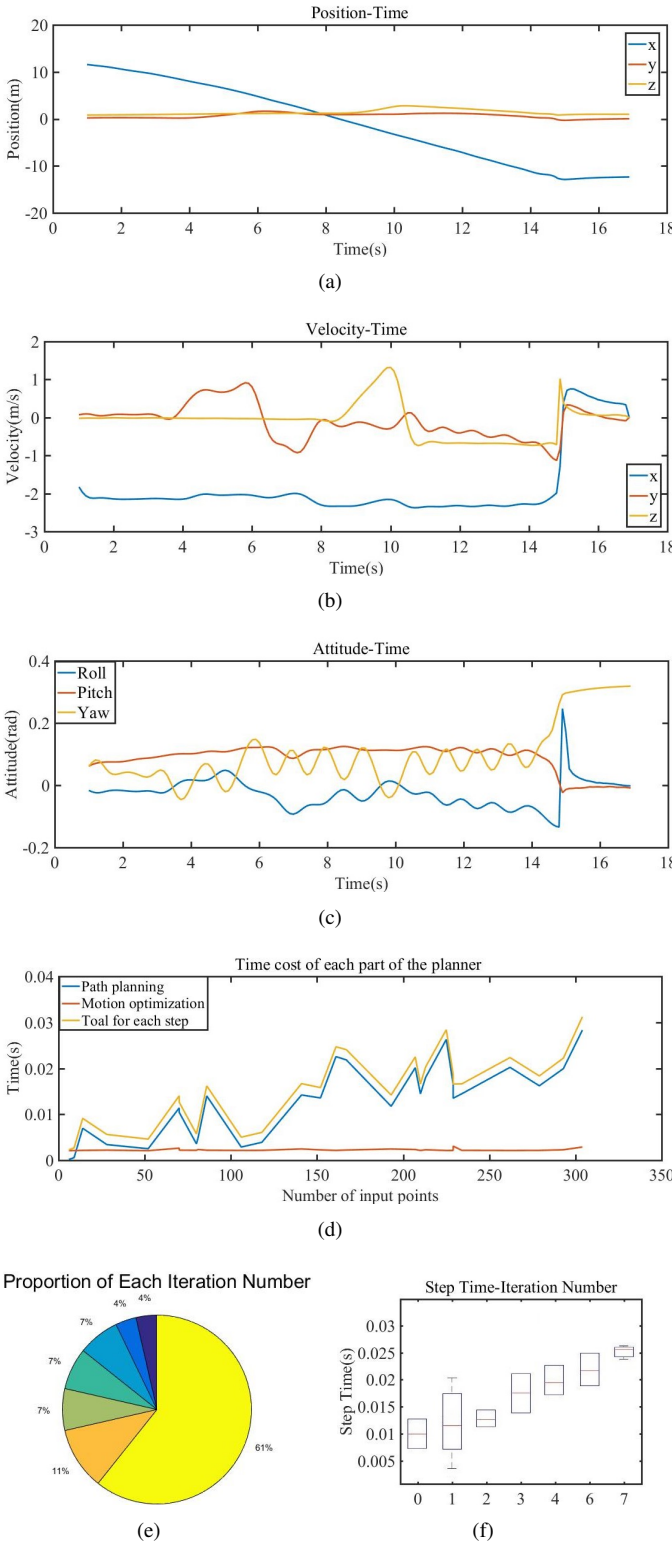


Fig. 8. (a)-(c): Curve of the three-axis coordinate position, flight speed, attitude angle; (d): curve of time cost of each part of the planner versus number of points in Pcl5; (e): pie chart for the proportion of each iteration number; (f): the boxplot of time cost for each iteration number.

because the drone was switched to position control mode when it is close enough( $<0.3$  m in this test) to the goal. We can see from the boxplot that the number of iteration time in the angular search is the major influential factor to the time cost, Fig. 8(e) shows that in most instances the HAS method can work out the feasible solution with less than 3 steps, so the average step time can be controlled within 20ms. The time cost also relates to the number of input points to some extent, which means we can decrease the time cost by simplifying the point cloud(Pcl5) in a more efficient way. In addition, there is still huge room for improvement by changing the code to C++, improving the hardware of the simulation platform.

## V. CONCLUSION

This work presented a trajectory planners framework based on the HAS method, for safe and quick responding flights in unknown environments. The key properties of this planner are that it uses a direct waypoint search method on a simplified point cloud to reduce the time cost and the safety is ensured by restricting  $d_{max} < r_{safe}$  by setting parameters and compromise on  $v_{max}$  and  $l_d$  when necessary. Our proposed planner was tested successfully in different simulation environments, achieving the average step time cost under 18ms. The time cost is believed to be able to achieve under 9ms on a higher performance hardware platform with C++ code.

## REFERENCES

- [1] F. E. Ducho et al., "Path Planning with Modified a Star Algorithm for a Mobile Robot," *Procedia Engineering*, vol. 96, pp. 59-69, 2014.
- [2] E. A., "Using occupancy grids for mobile robot perception and navigation," *Computer*, vol. 22, no. 6, pp. 46-57, 1989.
- [3] A. Hornung, K. M. Wurm, M. Bennewitz, C. Stachniss, and W. Burgard, "OctoMap: an efficient probabilistic 3D mapping framework based on octrees," *Autonomous Robots*, vol. 34, no. 3, pp. 189-206, 2013.
- [4] S. Choi, J. Park, E. Lim, and W. Yu, "Global path planning on uneven elevation maps," in *Ubiquitous Robots and Ambient Intelligence (URAI)*, 2012 9th International Conference on, 2012.
- [5] S. A. M. Coenen, J. J. M. Lunenburg, M. J. G. van de Molengraft and M. Steinbuch, "A representation method based on the probability of collision for safe robot navigation in domestic environments," 2014 IEEE/RSJ International Conference on Intelligent Robots and Systems, Chicago, IL, 2014, pp. 4177-4183.
- [6] B. T. Lopez and J. P. How, "Aggressive collision avoidance with limited field-of-view sensing," presented at the 2017 IEEE International Conference on Intelligent Robots and Systems (IROS), Vancouver, BC, 2017.
- [7] S. Liu, M. Watterson, S. Tang, and V. Kumar, "High speed navigation for quadrotors with limited onboard sensing" presented at the 2016 IEEE International Conference on Robotics and Automation (ICRA), Stockholm, 2016.
- [8] H. Chen, P. Lu and C. Xiao, "Dynamic Obstacle Avoidance for UAVs Using a Fast Trajectory Planning Approach," 2019 IEEE International Conference on Robotics and Biomimetics (ROBIO), Dali, China, 2019, pp. 1459-1464.
- [9] M. Watterson and V. Kumar, "Safe receding horizon control for aggressive MAV flight with limited range sensing," in 2015 IEEE/RSJ International Conference on Intelligent Robots and Systems (IROS), Hamburg, 2015, pp. 3235-3240.
- [10] van den Berg, J., Wilkie, D., Guy, S. J., Niethammer, M., & Manocha, D. (2012). LQG-obstacles: Feedback control with collision avoidance for mobile robots with motion and sensing uncertainty. *Proceedings of the IEEE International Conference on Robotics and Automation (ICRA)*, Saint. Paul, MN, 346-353.

[11] Helen Oleynikova, Zachary Taylor, Roland Siegwart, and Juan Nieto. Safe local exploration for replanning in cluttered unknown environments for microaerial vehicles. *IEEE Robotics and Automation Letters*, 3(3):1474-1481, 2018.

[12] M. W. Mueller, M. Hehn, and R. D'Andrea, "A Computationally Efficient Motion Primitive for Quadrocopter Trajectory Generation," *IEEE Transactions on Robotics*, vol. 31, no. 6, pp. 1-17, 2015.

[13] T. M. Howard, C. J. Green, A. Kelly, and D. Ferguson, State space sampling of feasible motions for high-performance mobile robot navigation in complex environments, *Journal of Field Robotics*, vol. 25, no. 6-7, pp. 325-345, 2008.

[14] B. Zhou, F. Gao, L. Wang, C. Liu, and S. Shen, "Robust and Efficient Quadrotor Trajectory Generation for Fast Autonomous Flight," *IEEE Robotics and Automation Letters*, vol. 4, 4, pp. 3529-3536, 2019.

[15] James A Preiss, Karol Hausman, Gaurav S Sukhatme, and Stephan Weiss. Trajectory optimization for self-calibration and navigation. In *Robotics: Science and Systems*, 2017.

[16] Bialkowski, Joshua, et al. Efficient Collision Checking in Sampling-Based Motion Planning via Safety Certificates. *The International Journal of Robotics Research*, vol. 35, no. 7, June 2016, pp. 767-796.

[17] Webb, D. J., & van den Berg, J. (2013).Kinodynamic RRT\*: Asymptotically optimal motion planning for robots with linear dynamics. *Proceedings of the IEEE International Conference on Robotics and Automation(ICRA)*, Germany, 5054-5061.

[18] Richter, C., Bry, A., & Roy, N. (2013).Polynomial trajectory planning for aggressive quadrotor flight in dense indoor environments. *Proceedings of the International Symposium of Robot. Research (ISRR)*,Singapore, 649-666.

[19] A. Majumdar, M. Tobenkin, and R. Tedrake, Algebraic verification for parameterized motion planning libraries, in *American Control Conference (ACC)*, 2012. IEEE, 2012, pp. 250-257.

[20] M. Burri, H. Oleynikova, M. W. Achtelik, and R. Siegwart, Real-time visual-inertial mapping, re-localization and planning onboard mavs in unknown environments in *Intelligent Robots and Systems (IROS)*, 2015 *IEEE/RSJ International Conference on*. IEEE, 2015, pp. 1872-1878.

[21] J. Chen, T. Liu, and S. Shen, Online generation of collision-free trajectories for quadrotor flight in unknown cluttered environments, in *2016 IEEE International Conference on Robotics and Automation (ICRA)*. IEEE, 2016, pp. 1476-1483.

[22] J. Tordesillas, B. T. Lopez and J. P. How, "FASTER: Fast and Safe Trajectory Planner for Flights in Unknown Environments," 2019 *IEEE/RSJ International Conference on Intelligent Robots and Systems (IROS)*, Macau, China, 2019, pp. 1934-1940.